Octacoordinate metal carbonyls of scandium and yttrium: Theoretical calculations and experimental observation

ARTICLE *in* RAPID COMMUNICATIONS IN MASS SPECTROMETRY · JUNE 2013

Impact Factor: 2.25 · DOI: 10.1002/rcm.6573 · Source: PubMed

Research Article

Rapid Communications in Mass Spectrometry

Received: 10 January 2013 Revised: 16 March 2013 Accepted: 17 March 2013 Published online in Wiley Online Library

Rapid Commun. Mass Spectrom. **2013**, 27, 1403–1409
(wileyonlinelibrary.com) DOI: 10.1002/rcm.6573

Octacoordinate metal carbonyls of scandium and yttrium: theoretical calculations and experimental observation

Xiaopeng Xing[1], Jie Wang[1], Hua Xie[2], Zhiling Liu[2], Zhengbo Qin[2], Lijuan Zhao[1] and Zichao Tang[2]*

[1]University of Chinese Academy of Sciences, College of Materials Sciences and Opto-Electronic Technology, Beijing 100049, China
[2]State Key Laboratory of Molecular Reaction Dynamics, Dalian Institute of Chemical Physics, Chinese Academy of Sciences, Dalian 116023, China

RATIONALE: The transition metal carbonyls are among the most important complexes in coordination chemistry. The maximum coordination number in these complexes is seven. Because the cations Sc^+ and Y^+ have empty second outermost *d* orbital subshells, they can possibly bond eight CO ligands, forming the 18-electron $d^{10}s^2p^6$ noble gas configuration. The aim of this study is to determine whether the octacoordinate metal carbonyls of Sc^+ and Y^+ exist.
METHODS: The structures and bonding of $M(CO)_n^+$ (M = Sc and Y, n = 7–9) were studied using Density Functional Theory (DFT) calculations with the functionals of B3LYP and BP86. The cationic complexes from laser ablation of Sc and Y in CO gas were analyzed by time-of-flight mass spectrometry.
RESULTS: The structures of $M(CO)_n^+$ (M = Sc and Y, n = 7–9) and the bond dissociation energies for the last CO ligand in $M(CO)_n^+$ (M = Sc and Y, n = 8 and 9) were obtained using DFT calculations. The products in the experiment for both metals include the series $MO(CO)_n^+$, $MO(H_2O)(CO)_n^+$ and $M(CO)_n^+$ (M = Sc or Y). The intensities of the $MO(CO)_n^+$ and $MO(H_2O)(CO)_n^+$ ions change gradually with the number of CO ligands, while most $M(CO)_n^+$ ions are very weak except for three intense ones, $Sc(CO)_7^+$, $Sc(CO)_8^+$ and $Y(CO)_8^+$.
CONCLUSIONS: Comparisons between the theoretical calculations and the experimental observations indicate that eight CO ligands are chemically bonded on the central atom in the singlet state of $Sc(CO)_8^+$ ($^1A_1$ state of D_{4d} symmetry) and the singlet and triplet states of $Y(CO)_8^+$ ($^1A_1$ state of D_{4d} symmetry and $^3A_{1g}$ state of O_h symmetry). The $^1A_1$ states of both $Sc(CO)_8^+$ and $Y(CO)_8^+$ have the 18-electron $d^{10}s^2p^6$ noble gas configuration. In $M(CO)_9^+$ (M = Sc or Y), the ninth CO is weakly adsorbed on the external shell. Copyright © 2013 John Wiley & Sons, Ltd.

Transition metal carbonyls have applications in the industrial field of homogeneous catalysis.[1] They are also prototypical models for many theoretical concepts including ligand field theory, 18-electron rule, orbital hybridizations and Dewar-Chatt-Duncanson bonding interaction.[2–4] These concepts laid the foundation of modern coordination chemistry. Early work on mononuclear transition metal carbonyls focused on the neutral species synthesized in the condensed phase, and the ionic transition metal carbonyls were subsequently isolated as salts with suitable counter ions.[2] With the development of techniques for gas-phase experiments and matrix-isolation, more saturated and unsaturated metal carbonyls have been generated and characterized. The typical experimental methods involved generating transition metal carbonyls through reactions of a single metal ion or atom with CO, and then characterizing the products using mass spectrometry, infrared dissociation spectroscopy and photoelectron spectroscopy in the gas phase,[5–13] or infrared absorption spectroscopy in matrix.[3,14–18] At the same time, Density Functional Theory (DFT) calculations combined with the experiments have been effective in predicting the structures and bonding of these complexes.

Except a very few special species,[5] most saturated transition metal carbonyls satisfy the 18-electron rule, in which the electrons from the central metal atom and the ligands form the $d^{10}s^2p^6$ noble gas configuration. Typical examples include neutral $Ni(CO)_4$, $Fe(CO)_5$ and $Cr(CO)_6$, and the cationic $Cu(CO)_4^+$, $Co(CO)_5^+$ and $Mn(CO)_6^+$.[2,3,8,19,20] According to this 18-electron rule, early transition metals are expected to bond with more CO ligands, since they have fewer *d* electrons. However, the maximum coordination numbers in many transition metal carbonyls was thought to be six.[3] For example, $Ti(CO)_n$ (n = 2–6) were found in matrix, while $Ti(CO)_7$ was not observed despite its possible 18-electron configuration.[21] Recently, some heptacoordinate metal carbonyls have been reported. For example, $M(CO)_7^+$ (M = V, Nb and Ta) were generated using laser vaporization and characterized by infrared dissociation spectroscopy in the gas phase;[22] theoretical calculations predicted that $M(CO)_7$ (M = Ti, Zr and Hf)[23] and $Sc(CO)_7^{0/-}$[24] should be stable enough to be experimentally observed. Till now, $U(CO)_8^+$ is the only octacoordinate metal carbonyl that has been reported,[25] where uranium belongs to the actinide group.

* *Correspondence to:* Z. C. Tang, State Key Laboratory of Molecular Reaction Dynamics, Dalian Institute of Chemical Physics, Chinese Academy of Sciences, Dalian 116023, China. E-mail: zctang@dicp.ac.cn

In this communication, we present theoretical calculations and experimental clues for the stabilities of $Sc(CO)_8^+$ and $Y(CO)_8^+$, in which eight CO ligands are directly bonded on the Sc or Y atom. The lowest energy structure of $Sc(CO)_8^+$ was predicted to be a singlet D_{4d} geometry, while the two structures of $Y(CO)_8^+$, a singlet D_{4d} geometry and a triplet O_h geometry, have nearly identical energies. Like the traditional tetracoordinate and hexacoordinate transitional metal carbonyls, these octacoordinate species could be new model systems for fundamental concepts in inorganic and organometallic chemistry.

COMPUTATIONAL METHODS

DFT calculations were carried out to study the structures and bonding of $M(CO)_n^+$ (M = Sc and Y, n = 7–9). Both the singlet and the triplet states of these complexes were considered. We initially optimized their structures using the B3LYP method with Lanl2dz basis sets for all elements. The optimizations of each species started from several points, including the structures with all CO ligands bonded on the central atom and those with one CO ligand adsorbed on the second shell. The obtained structures were further optimized using two sophisticated theoretical approaches. One still used the B3LYP method while the other used the BP86 method. In both approaches, 6-311+G (3df) basis sets were selected for Sc, C and O, and the SDD (SC-RECP, MWB28) basis set was selected for Y. In all calculations, frequency analysis was applied to ensure that the obtained structures are real minima. The relative energies from the two sophisticated calculations were used to compute the dissociation energies of the last CO ligand in $M(CO)_n^+$ (M = Sc and Y, n = 8 and 9). All calculations were performed using the Gaussian 09 program.[26]

EXPERIMENTAL

The experiments were carried out on a home-made instrument designed to take photoelectron imaging spectra of anionic clusters, as has been described elsewhere.[27,28] Briefly, the instrument includes a laser vaporization ion source, a reflectron time-of-flight (TOF) mass spectrometer and a collinear velocity-map photoelectron imaging analyzer. Only the ion source and the mass spectrometer were used in this study. The ion source is similar to that originally designed by Smalley and co-workers,[29,30] and has been used to study the reactions of clusters or atomic ions with gas molecular in our previous studies.[31–37] Figure 1 shows the details of this ion source and the accelerator of the TOF mass spectrometer built according to the Wiley-McLaren design.[38]

In these experiments, the metal cations were generated by laser vaporization of the rotating metal target, and then reacted with CO to form various complexes. The temperature inside the growth channel should be equal to that of the walls of the instrument, which was about 300 K. The pressure in this region was close to that in the foreline, which was 10 atm. The generated species were cooled by supersonic expansion through the nozzle. Their final temperature can be estimated according to the simulations on the vibrationally resolved photoelectron spectra of the generated anionic clusters. After considering the uncertainties in the experiments and the simulations, the temperature of the species from this source was estimated to be within the range 120–180 K.[39–41] The pressure after supersonic expansion can be roughly calculated using the equation describing adiabatic isentropic processes:

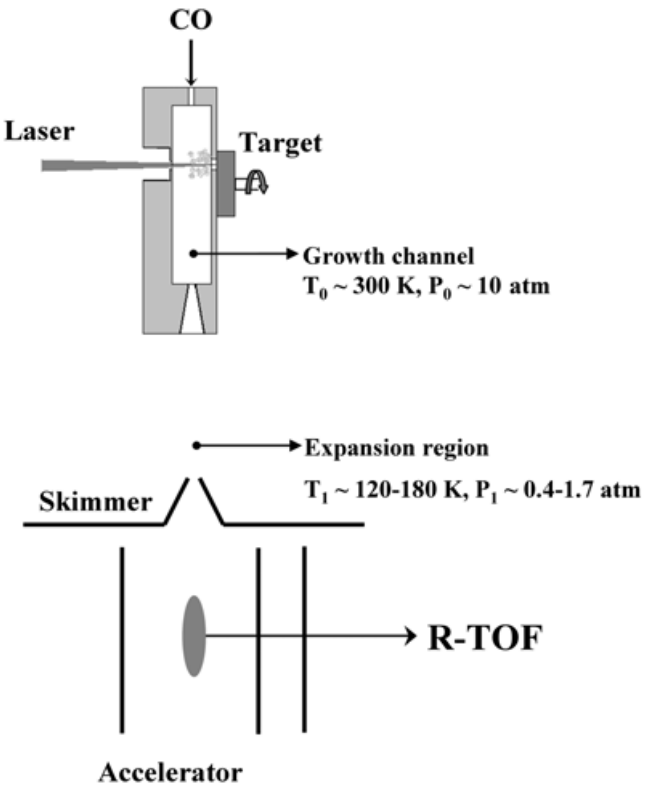

Figure 1. The laser vaporization ion source and the accelerator of the time-of-flight mass spectrometer.

$$\frac{T_1}{T_0} = \left(\frac{P_1}{P_0}\right)^{(\gamma-1)/\gamma} \quad (1)$$

where γ is the heat capacity ratio C_p/C_v, which equals 1.4 for the diatomic CO. As shown in Fig. 1, the T_1 value of 120–180 K corresponds to a P_1 value of 0.40–1.7 atm when T_0 and P_0 equal 300 K and 10 atm, respectively, in the growth channel.

After supersonic expansion, the cationic products went through the skimmer between the source chamber and the TOF chamber, and entered the accelerating region perpendicularly. They were accelerated by a pulse voltage of 1.2 kV, reflected by the reflectron, and then detected using a multi-channel plate detector. The ion signals were recorded by a 12 bit analog-to-digital conversion card and processed by a PC computer. Each spectrum was the accumulation of about 500 laser shots at 10 Hz repetition rate. The TOF mass spectrometer was calibrated using the metal cations of Sc^+, Ag^+ and Au^+ generated by laser vaporization of the metals in helium gas.

RESULTS AND DISCUSSION

Theoretical calculations of $M(CO)_n^+$ (M = Sc and Y, n = 7–9)

Figures 2 and 3 display the theoretical geometries of $Sc(CO)_{7-9}^+$ and $Y(CO)_{7-9}^+$, respectively. Their symmetries, electronic states, relative energies and bond lengths are also indicated.

Rapid Communications in Mass Spectrometry

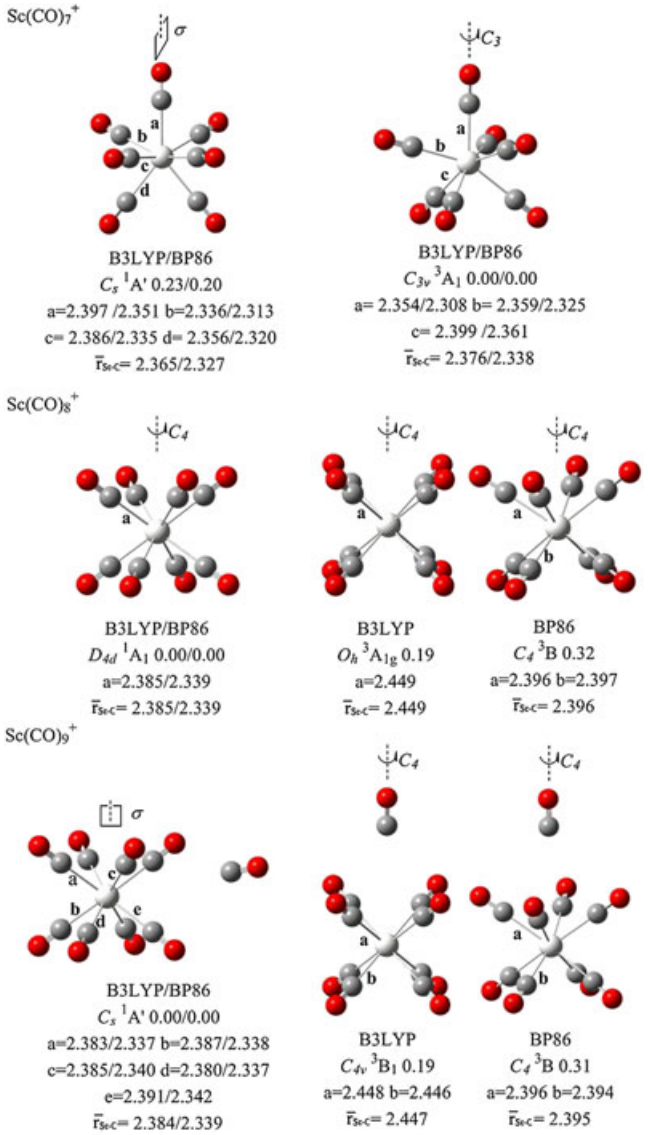

Figure 2. Optimized structures for the singlet states (left column) and the triplet states (right column) of $Sc(CO)_n^+$ ($n = 7$, 8 and 9). The symmetries, the electronic states, the relative energies (in eV) and the metal-carbon bond lengths (in Å) based on both B3LYP and BP86 methods are indicated.

As shown in Fig. 2, a *Cs* geometry with the $^1A'$ state and a C_{3v} geometry with the $^3A_1$ state were predicted for $Sc(CO)_7^+$, with the C_{3v} geometry being lower in energy. The singlet $Sc(CO)_8^+$ was determined to be D_{4d} geometry with the $^1A_1$ state based on both the B3LYP and the BP86 methods, while the triplet one was predicted to be O_h geometry with the $^3A_{1g}$ state at the B3LYP level and a C_4 geometry with the ^3B state at the BP86 level. The singlet D_{4d} geometry is determined to be the lowest-lying structure for $Sc(CO)_8^+$ based on two theoretical methods. For $Sc(CO)_9^+$, the predicted structures for both the singlet state and the triplet state have a weakly bonded CO onto the corresponding structures of $Sc(CO)_8^+$. For all optimized structures of $Sc(CO)_{7,8,9}^+$, the Sc–C bond lengths from the B3LYP method are slightly longer than the corresponding ones from the BP86 method, and the average Sc–C bond lengths of a singlet structure are shorter than those of the corresponding triplet one.

As shown in Fig. 3, the calculations using both B3LYP and BP86 methods obtained consistent geometries for all $Y(CO)_{7-9}^+$ ions. A C_s geometry with the $^1A'$ state and a C_{3v} geometry with the $^3A_1$ state were predicted for the singlet and triplet $Y(CO)_7^+$, respectively. The triplet C_{3v} geometry is lower in energy at both B3LYP and BP86 levels. The singlet and the triplet states of $Y(CO)_8^+$ are D_{4d} geometry with the $^1A_1$ state and O_h geometry with the $^3A_{1g}$ state, respectively. Their energies are nearly identical based on the two theoretical methods. In the predicted structures of $Y(CO)_9^+$, the last CO is weakly bonded onto the second shell of the corresponding structures of $Y(CO)_8^+$. Similarly to the results of the scandium carbonyls, the Y–C bond lengths from the B3LYP method are slightly longer than the corresponding ones from the BP86

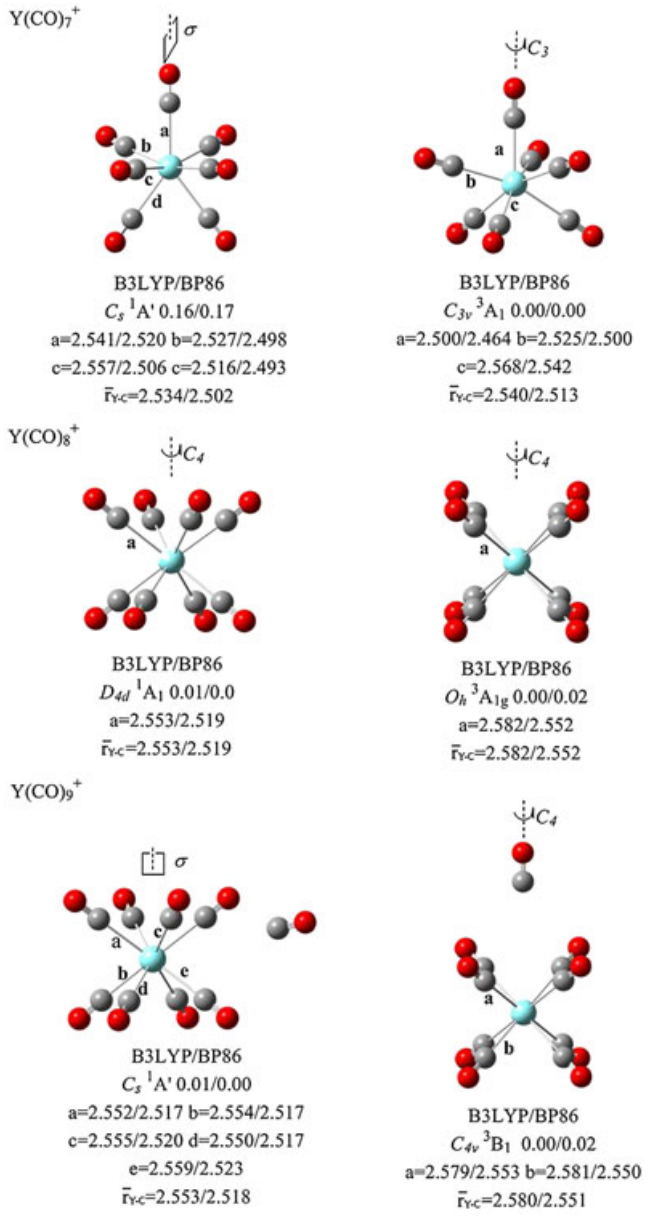

Figure 3. Optimized structures for the singlet states (left column) and the triplet states (right column) of $Y(CO)_n^+$ ($n = 7$, 8 and 9). The symmetries, electronic states, relative energies (in eV) and the metal–carbon bond lengths (in Å) based on both B3LYP and BP86 methods are indicated.

method; the singlet structure has shorter Y–C bonds than the corresponding triplet one for each species. For the similar structures and electronic states, the metal–carbon bond lengths in $Y(CO)_{7,8,9}^+$ are obviously longer than those in $Sc(CO)_{7,8,9}^+$.

We also computed the bond dissociation energies of $M(CO)_n^+$ (M = Sc and Y, n = 8 and 9), corresponding to the products being one CO and the $M(CO)_{n-1}^+$ with the spin multiplicity of the parent. The computed bond dissociation energies and the calculation results from Figs. 2 and 3 are summarized in Table 1.

Metal carbonyls of Sc and Y from laser vaporization in CO

In these experiments, CO molecules can react very quickly with the metal species in the growth channel, preventing them from growing to large clusters. Figures 4 and 5 display the cationic products from laser vaporization of Sc and Y in 10 atm CO, respectively. The dominant products contain only one metal atom.

The main products in Fig. 4 were identified as $ScO(CO)_n^+$ (n = 1–7), $ScO(H_2O)(CO)_n^+$ (n = 2–7) and $Sc(CO)_n^+$ (n = 3–8). Among the four elements in these species, Sc and H have only one natural isotope, while the natural abundances of ^{13}C and ^{18}O are about 1.1% and 0.2% of the dominant ^{12}C and ^{16}O, respectively. As an example, the insert shows the isotopic peaks of $Sc(CO)_7^+$. According to theoretical simulations, four peaks of $Sc(CO)_7^+$ have intensities that are not lower than 0.1% of the highest one. The ions are *m/z* 241, 242, 243 and 244, and their relative intensities are 100, 7.9, 1.6 and 0.1, respectively. The spectrum and the simulation are qualitatively consistent, except that the experimental intensities of the three heavier peaks seem a little stronger than their theoretical values. This discrepancy could be caused by the background from the oscillations of the detection circuit following the strong peak. The most surprising finding in Fig. 4 relates to the $Sc(CO)_n^+$ series, in which $Sc(CO)_7^+$ and $Sc(CO)_8^+$ are relatively intense and the other members are extremely weak. We also found that the ratio of $Sc(CO)_7^+$ and $Sc(CO)_8^+$ is independent of the CO pressure. The extra oxygen atoms in $ScO(CO)_n^+$ or $ScO(H_2O)(CO)_n^+$ could come from the dissociation of CO in the vaporization process and the H_2O in $ScO(H_2O)(CO)_n^+$ should be from moisture in the system. It has been shown that trace amounts of H_2O can act as electron scavengers and this obviously increases the intensities of cationic products in laser vaporization.[42] The intensities of $ScO(CO)_n^+$ and $ScO(H_2O)(CO)_n^+$ change gradually with the number of CO ligands.

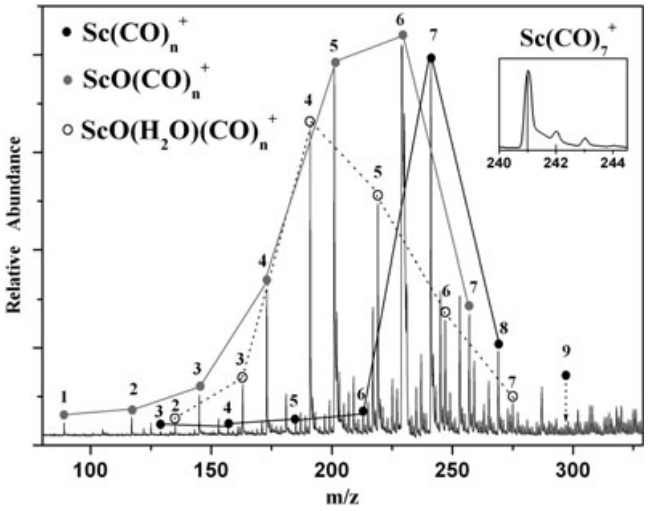

Figure 4. Mass spectrum of the cationic products from laser vaporization of Sc in high pressure CO. Three dominant series, $Sc(CO)_n^+$, $ScO(CO)_n^+$ and $ScO(H_2O)(CO)_n^+$, are indicated. The insert shows the experimental and simulated peaks of $Sc(CO)_7^+$.

Table 1. The electronic states, electronic configurations, symmetries and relative energies of the singlet and triplet states of $M(CO)_n^+$ (M = Sc and Y, n = 7–9). The bonding energies of the last CO in the singlet and triplet states of $M(CO)_n^+$ (M = Sc and Y, n = 8 and 9) are also indicated

			B3LYP			BP86		
Complex	Electronic state[a]	Electronic configuration[a]	Symmetry	ΔE (eV)	Eb (eV)[b]	Symmetry	ΔE (eV)	Eb (eV)[b]
$Sc(CO)_7^+$	$^1A'$	$\ldots a''^2a'^2a''^2a'^2$	C_s	0.23		C_s	0.20	
	$^3A_1$	$\ldots e^2e^2a_1^2e^1e^1$	C_{3v}	0.00		C_{3v}	0.00	
$Sc(CO)_8^+$	$^1A_1$	$\ldots e_3^2e_2^2e_2^2a_1^2$	D_{4d}	0.00	0.39	D_{4d}	0.00	0.59
	$^3A_{1g}/^3B$	$\ldots t_{2g}^2t_{2g}^2a_{2u}^2e_g^1e_g^1/\ \ldots e^2b^2b^2a^1b^1$	O_h	0.19	−0.03	C_4	0.32	0.07
$Sc(CO)_9^+$	$^1A'$	$\ldots a'^2a''^2a'^2a'^2$	C_s	0.00	0.06	C_s	0.00	0.04
	$^3B_1/^3B$	$\ldots b_2^2b_2^2a_1^2b_1^1a_1^1/\ \ldots b^2b^2a^2a^1b^1$	C_{4v}	0.19	0.06	C_4	0.31	0.05
$Y(CO)_7^+$	$^1A'$	$\ldots a''^2a'^2a''^2a'^2$	C_s	0.16		C_s	0.17	
	$^3A_1$	$\ldots e^2a_1^2a_1^2e^1e^1$	C_{3v}	0.00		C_{3v}	0.00	
$Y(CO)_8^+$	$^1A_1$	$\ldots e_1^2e_2^2e_2^2a_1^2$	D_{4d}	0.01	0.51	D_{4d}	0.00	0.64
	$^3A_{1g}$	$\ldots t_{2g}^2t_{2g}^2a_{2u}^2e_g^1e_g^1$	O_h	0.00	0.36	O_h	0.02	0.45
$Y(CO)_9^+$	$^1A'$	$\ldots a'^2a''^2a'^2a'^2$	C_s	0.01	0.06	C_s	0.00	0.04
	$^3B_1$	$\ldots b_2^2b_2^2a_1^2b_1^1a_1^1$	C_{4v}	0.00	0.06	C_{4v}	0.02	0.05

[a]For the triplet $Sc(CO)_8^+$ and $Sc(CO)_9^+$, the two electronic states and configurations correspond to the two geometries from the B3LYP and BP86 methods, respectively.
[b]The bond energy (Eb) corresponds to dissociation from $M(CO)_n^+$ to $M(CO)_{n-1}^+$, in which the spin multiplicity does not change.

Rapid Communications in Mass Spectrometry

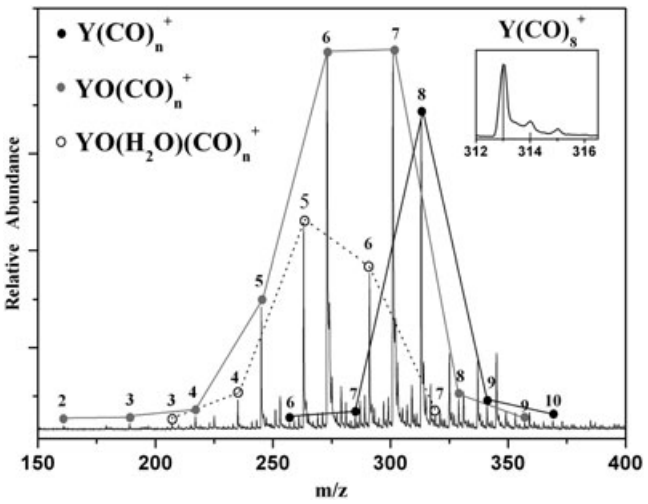

Figure 5. Mass spectrum of the cationic products from laser vaporization of Y in high pressure CO. Three dominant series, $Y(CO)_n^+$, $YO(CO)_n^+$ and $YO(H_2O)(CO)_n^+$, are indicated. The insert shows the experimental and simulated peaks of $Y(CO)_8^+$.

In Fig. 5, the dominant series $YO(CO)_n^+$ (n = 2–9), $YO(H_2O)(CO)_n^+$ (n = 3–7) and $Y(CO)_n^+$ (n = 6–10) were identified. Similarly to the scandium complexes shown in Fig. 4, each product of yttrium also has several isotopic peaks caused by ^{13}C and ^{18}O. The insert in Fig. 5 displays the enlarged spectrum of $Y(CO)_8^+$, showing the comparison between the simulation and the experiments. Theoretically, the four detectable ions for $Y(CO)_8^+$ are m/z 313, 314, 315 and 316 Da, and their relative intensities are 100, 9, 1.9 and 0.1, respectively. This is qualitatively consistent with the experimental spectrum in the insert. In contrast to the gradual change in the intensities of $YO(CO)_n^+$ and $YO(H_2O)(CO)_n^+$, most of the $Y(CO)_n^+$ ions are very weak except for $Y(CO)_8^+$. The extra O atom and the H_2O in the products should also come from the dissociation of CO in the vaporization process and the background moisture.

Comparisons between theoretical calculations and experimental observations

The CO adsorption or elimination will be relatively slow if the spin multiplicity changes.[16–18] In calculations, we only considered the bond energies corresponding to the processes with spin conservation. As shown in Table 1, the data from B3LYP and BP86 methods are qualitatively consistent. The $^1A'$ state of $Sc(CO)_7^+$ can adsorb one CO, forming the $^1A_1$ state of $Sc(CO)_8^+$ and releasing a few tenths of eV, while the bonding energy of one CO on the $^3A_1$ state of $Sc(CO)_7^+$ is less than 0.1 eV, which is similar to the adsorption strength of the CO on the external shell. The last CO in the singlet or triplet state of $Sc(CO)_9^+$ is weakly adsorbed on the external shell. The bond energies of the last CO in both $^1A_1$ and $^3A_{1g}$ states of $Y(CO)_8^+$ are a few tenths of eV, and the last CO in the $^1A'$ or $^3B_1$ state of $Y(CO)_9^+$ is on the external shell, and the theoretical bond strength is less than 0.1 eV.

The bond energies of the last CO in $M(CO)_{8,9}^+$ (Sc and Y) predicted by calculations are supported by the experimental mass spectra shown in Figs. 4 and 5. The estimated temperatures in these experiments were higher than those of the species from many other sources.[5,7,43,44] This is in line with the argument that the expansion cooling in the traditional Smalley-type cluster source is not as efficient as that of the so-called cutaway design or the source using helium as the carrier gas.[42] Equations (2) and (3) are the adsorption process and its van't Hoff equation, respectively:

$$M(CO)_{n-1}^+ + CO = M(CO)_n^+ \quad (2)$$

$$\ln K = \ln \frac{[M(CO)_n^+]}{[M(CO)_{n-1}^+] \times \frac{P_{co}}{P^\Theta}} = -\frac{\Delta_r H^\Theta}{RT} + \frac{\Delta_r S^\Theta}{R} \quad (3)$$

According to the experimental measurements on the clusters of $(CO)_n^+$,[45] $H^+(CO)_n$[46] and $CF_3^+(CO)_n$,[47] the $\Delta_r S^\Theta$ and $\Delta_r H^\Theta$ corresponding to adsorbing CO on the external shell are around −100 J.mol^{-1}.K^{-1} and less than 10 KJ.mol^{-1} (~0.1 eV), respectively. It is reasonable to assume that the $\Delta_r S^\Theta$ and $\Delta_r H^\Theta$ values for the adsorption of CO on the external shell of $M(CO)_n^+$ are similar. The ratios $\frac{[M(CO)_n^+]}{[M(CO)_{n-1}^+]}$ in Eqn. (3) were then calculated to be less than 1/304, 1/124 and 1/19 when P_{co} and T were 10 atm CO and 300 K (in the growth channel), 1.7 atm CO and 180 K (the high limits after expansion cooling), and 0.4 atm and 120 K (the low limits after expansion cooling), respectively. This implies that the equilibrium concentration of $M(CO)_n^+$ should be less than 1/19 of that of its neighbor, $M(CO)_{n-1}^+$, if the last CO is on its external shell. As shown in Figs. 4 and 5, it is likely that $Sc(CO)_9^+$ and $Y(CO)_9^+$ contain the weakly adsorbed CO, while the intense $Sc(CO)_7^+$, $Sc(CO)_8^+$ and $Y(CO)_8^+$ do not. This observation is consistent with the calculation results that the last COs in the lowest-lying states of both $Sc(CO)_9^+$ and $Y(CO)_9^+$ and the triplet state of $Sc(CO)_8^+$ are weakly bonded (Eb <0.1 eV), while the last COs in the singlet state of $Sc(CO)_8^+$ and the singlet or triplet state of $Y(CO)_8^+$ are more strongly bonded (Eb = 0.35–0.65 eV).

Overall, the comparisons between the calculations and experiments provide evidence for the stabilities of octacoordinate metal carbonyls of Sc and Y. The total numbers of electrons from their central metal atom and the CO ligands are eighteen in $M(CO)_8^+$ (M = Sc and Y), and these species therefore should form $d^{10}s^2p^6$ noble gas configuration in their $^1A_1$ states. The bond dissociation energies of the last CO in the $^1A_1$ states of $M(CO)_8^+$ (M = Sc and Y) are comparable with those of $Cu(CO)_4^+$ (0.55 eV),[48] $Ag(CO)_4^+$ (0.47 eV),[48] $Co(CO)_5^+$ (0.78 eV),[49] etc. This indicates that the bonding in these $Sc(CO)_8^+$ or $Y(CO)_8^+$ complexes also belongs to chemical coordination.

CONCLUSIONS

The structures and bonding of $M(CO)_{7-9}^+$ (M = Sc and Y) were studied using DFT calculations, and four stable carbonyl complexes were predicted: the C_{3v} geometry of $Sc(CO)_7^+$ with the $^3A_1$ state, the D_{4d} geometry of $Sc(CO)_8^+$ with the $^1A_1$ state, the O_h geometry of $Y(CO)_8^+$ with the $^3A_{1g}$ state and the D_{4d} geometry of $Y(CO)_8^+$ with the $^1A_1$ state. The cationic products from laser vaporization of Sc and Y in high-pressure CO were analyzed using time-of-flight mass spectrometry, and the dominant series, $MO(CO)_n^+$, $MO(H_2O)(CO)_n^+$ and $M(CO)_n^+$ (M = Sc or Y), were observed. The intensities of $MO(CO)_n^+$

and $MO(H_2O)(CO)_n^+$ vary gradually with the number of CO ligands. However, the intensities of most $M(CO)_n^+$ ions are very weak except for the relatively intense $Sc(CO)_7^+$, $Sc(CO)_8^+$ and $Y(CO)_8^+$. This observation is consistent with the theoretical predictions. These calculations and experiments provide evidence for the stabilities of the octacoordinate carbonyls of Sc and Y, which have never been reported for any other transition metals. We note that the present experiments may only give a clue to the calculations, and further investigation using infrared spectroscopy would be able to confirm the predicted structures and electronic states of these model complexes.

Acknowledgements

This work was supported by the National Natural Science Foundation of China (Grant Nos. 21073186, 21103186, 21103226 and 21273278), the Ministry of Science and Technology of China, and the Chinese Academy of Sciences. The calculated results reported in this paper were obtained on the Deepcomp7000 of Supercomputing Center, Computer Network Information Center of Chinese Academy of Sciences.

REFERENCES

[1] J. F. Hartwig, *Organotransition Metal Chemistry: From Bonding to Catalysis*. University Science Books, Sausalito, CA, **2010**.
[2] F. A. Cotton, G. Wilkinson, C. A. Murillo, M. Bochmann. *Advanced Inorganic Chemistry*, (6th edn.), John Wiley, New York, **1999**.
[3] M. F. Zhou, L. Andrews, C. W. Bauschlicher. Spectroscopic and theoretical investigations of vibrational frequencies in binary unsaturated transition-metal carbonyl cations, neutrals, and anions. *Chem. Rev.* **2001**, *101*, 1931.
[4] G. Frenking, N. Frohlich. The nature of the bonding in transition-metal compounds. *Chem. Rev.* **2000**, *100*, 717.
[5] C. Chi, J. Cui, X. Xing, G. Wang, Z.-P. Liu, M. Zhou. Infrared photodissociation spectroscopy of trigonal bipyramidal 19-electron $Ni(CO)_5^+$ cation. *Chem. Phy. Lett.* **2012**, *542*, 33.
[6] G. Wang, C. Chi, J. Cui, X. Xing, M. Zhou. Infrared photodissociation spectroscopy of mononuclear iron carbonyl anions. *J. Phys. Chem. A* **2012**, *116*, 2484.
[7] A. D. Brathwaite, Z. D. Reed, M. A. Duncan. Infrared photodissociation spectroscopy of copper carbonyl cations. *J. Phys. Chem. A* **2011**, *115*, 10461.
[8] A. M. Ricks, Z. E. Reed, M. A. Duncan. Infrared spectroscopy of mass-selected metal carbonyl cations. *J. Mol. Spectros.* **2011**, *266*, 63.
[9] G. S. IckingKonert, H. Handschuh, G. Gantefor, W. Eberhardt. Bonding of CO to metal particles: Photoelectron spectra of $Ni_n(CO)_m^-$ and $Pt_n(CO)_m^-$ clusters. *Phys. Rev. Lett.* **1996**, *76*, 1047.
[10] C. P. G. Butcher, B. F. G. Johnson, J. S. McIndoe, X. Yang, X. B. Wang, L. S. Wang. Collision-induced dissociation and photodetachment of singly and doubly charged anionic polynuclear transition metal carbonyl clusters: $Ru_3Co(CO)_{13}^-$, $Ru_6C(CO)_{16}^{2-}$, and $Ru_6(CO)_{18}^{2-}$. *J. Chem. Phys.* **2002**, *116*, 6560.
[11] B. Chatterjee, F. A. Akin, C. C. Jarrold, K. Raghavachari. A comparison of stable carbonyls formed in the gas-phase reaction between group 10 atomic anions and methanol or methoxy radicals: Anion photoelectron spectroscopy and density functional theory calculations on $HNiCO^-$, $PdCO^-$, and $PtCO^-$. *J. Chem. Phys.* **2003**, *119*, 10591.
[12] Y.-L. Wang, H.-J. Zhai, L. Xu, J. Li, L.-S. Wang. Vibrationally resolved photoelectron spectroscopy of di-gold carbonyl clusters $Au_2(CO)_n^-$ (n = 1–3): Experiment and theory. *J. Phys. Chem. A* **2010**, *114*, 1247.
[13] Z. Liu, H. Xie, Z. Qin, R. Cong, X. Wu, Z. Tang, X. Lu, J. He. Vibrationally resolved photoelectron imaging of platinum carbonyl anion $Pt(CO)_n^-$ (n = 1–3): Experiment and theory. *J. Chem. Phys.* **2012**, *137*, 4302.
[14] L. Andrews, M. F. Zhou, X. F. Wang, C. W. Bauschlicher. Matrix infrared spectra and density functional calculations of manganese and rhenium carbonyl neutral and anion complexes. *J. Phys. Chem. A* **2000**, *104*, 8887.
[15] Z. Song, X. Wang. Ruthenium and osmium carbonyl nitrosyl complexes: Matrix infrared spectra and density functional calculations for $M(CO)_2(NO)_2$ and $M(CO)(NO)$ (M = Ru, Os). *Chem. Phys.* **2012**, *407*, 134.
[16] M. F. Zhou, L. Andrews. Matrix infrared spectra and density functional calculations of ScCO, $ScCO^-$, and $ScCO^+$. *J. Phys. Chem. A* **1999**, *103*, 2964.
[17] L. Jiang, Q. Xu. Reactions of laser-ablated la and y atoms with CO: Matrix infrared spectra and DFT calculations of the $M(CO)_x$ and MCO^+ (M = La, Y; x = 1–4) molecules. *J. Phys. Chem. A* **2007**, *111*, 3271.
[18] W. H. Xu, X. Jin, M. H. Chen, P. Pyykko, M. F. Zhou, J. Li. Rare-earth monocarbonyls MCO: comprehensive infrared observations and a transparent theoretical interpretation for M = Sc; Y; La-Lu. *Chem. Sci.* **2012**, *3*, 1548.
[19] F. Aubke, C. Wang. Carbon-monoxide as a sigma-donor ligand in coordination chemistry. *Coord. Chem. Rev.* **1994**, *137*, 483.
[20] M. Wrighton. Photochemistry of metal-carbonyls. *Chem. Rev.* **1974**, *74*, 401.
[21] M. F. Zhou, L. Andrews. Infrared spectra and density functional calculations of small vanadium and titanium carbonyl molecules and anions in solid neon. *J. Phys. Chem. A* **1999**, *103*, 5259.
[22] A. M. Ricks, Z. D. Reed, M. A. Duncan. Seven-coordinate homoleptic metal carbonyls in the gas phase. *J. Am. Chem. Soc.* **2009**, *131*, 9176.
[23] Q. Luo, Q.-S. Li, Z. H. Yu, Y. Xie, R. B. King, H. F. Schaefer, III. Bonding of seven carbonyl groups to a single metal atom: Theoretical study of $M(CO)_n$ (M = Ti, Zr, Hf; n = 7, 6, 5, 4). *J. Am. Chem. Soc.* **2008**, *130*, 7756.
[24] S.-M. Gao, W.-P. Guo, L. Jin, Y.-H. Ding. Maximum carbonyl-coordination number of scandium. Computational study of $Sc(CO)_n$ (n = 1–7), $Sc(CO)_7^-$ and $Sc(CO)_6^{3-}$. *Int. J. Quantum Chem.* **2013**, *113*, 1192.
[25] A. M. Ricks, L. Gagliardi, M. A. Duncan. Infrared spectroscopy of extreme coordination: The carbonyls of U^+ and UO_2^+. *J. Am. Chem. Soc.* **2010**, *132*, 15905.
[26] M. J. Frisch, G. W. Trucks, H. B. Schlegel, G. E. Scuseria, M. A. Robb, J. R. Cheeseman, G. Scalmani, V. Barone, B. Mennucci, G. A. Petersson, H. Nakatsuji, M. Caricato, X. Li, H. P. Hratchian, A. F. Izmaylov, J. Bloino, G. Zheng, J. L. Sonnenberg, M. Hada, M. Ehara, K. Toyota, R. Fukuda, J. Hasegawa, M. Ishida, T. Nakajima, Y. Honda, O. Kitao, H. Nakai, T. Vreven, J. A. Montgomery, Jr., J. E. Peralta, F. Ogliaro, M. Bearpark, J. J. Heyd, E. Brothers, K. N. Kudin, V. N. Staroverov, R. Kobayashi, J. Normand, K. Raghavachari, A. Rendell, J. C. Burant, S. S. Iyengar, J. Tomasi, M. Cossi, N. Rega, J. M. Millam, M. Klene, J. E. Knox, J. B. Cross, V. Bakken, C. Adamo, J. Jaramillo, R. Gomperts, R. E. Stratmann, O. Yazyev, A. J. Austin, R. Cammi, C. Pomelli, J. W. Ochterski, R. L. Martin, K. Morokuma, V. G. Zakrzewski, G. A. Voth, P. Salvador, J. J. Dannenberg, S. Dapprich, A. D. Daniels, Ö. Farkas, J. B. Foresman, J. V. Ortiz, J. Cioslowski, D. J. Fox. *Gaussian 09, Revision A02*, Gaussian, Inc., Wallingford, CT, **2009**.

[27] X. Wu, Z. Qin, H. Xie, R. Cong, X. Wu, Z. Tang, H. Fan. Vibrationally resolved photoelectron imaging of gold hydride cluster anions: AuH^- and Au_2H^-. *J. Chem. Phys.* **2010**, *133*, 044303.
[28] X. Wu, Z.-b. Qin, H. Xie, X.-h. Wu, R. Cong, Z.-c. Tang. Collinear velocity-map photoelectron imaging spectrometer for cluster anions. *Chin. J. Chem. Phys.* **2010**, *23*, 373.
[29] T. G. Dietz, M. A. Duncan, D. E. Powers, R. E. Smalley. Laser production of supersonic metal cluster beams. *J. Chem. Phys.* **1981**, *74*, 6511.
[30] L. S. Zheng, P. J. Brucat, C. L. Pettiette, S. Yang, R. E. Smalley. Formation and photodetachment of cold metal cluster negative-ions. *J. Chem. Phys.* **1985**, *83*, 4273.
[31] X. P. Xing, H. T. Liu, Z. C. Tang. Generation of M_m-phenyl$^-$ (M = Mn-Cu) complexes in the gas phase: Metal cluster anions inducement of a selective benzene C-H cleavage. *Physchemcomm* **2003**, *6*, 32.
[32] Z. X. Tian, X. P. Xing, Z. C. Tang. Reactions of lead cluster ions with ethylene, propene, *trans*-butene, and *cis*-butene. *Rapid Commun. Mass Spectrom.* **2002**, *16*, 1515.
[33] Z. X. Tian, X. P. Xing, Z. C. Tang. Reactions of lead cluster ions with acetone. *Rapid Commun. Mass Spectrom.* **2003**, *17*, 17.
[34] X. P. Xing, Z. X. Tian, H. T. Liu, Z. C. Tang. Reactions between M^+ (M = Si, Ge, Sn and Pb) and benzene in the gas phase. *Rapid Commun. Mass Spectrom.* **2003**, *17*, 1743.
[35] X. P. Xing, Z. X. Tian, H. T. Liu, Z. C. Tang. A comparative study of cation and anion cluster reaction products: The reaction mechanisms of lead clusters with benzene in gas phase. *J. Phys. Chem A* **2003**, *107*, 8484.
[36] H. T. Liu, S. T. Sun, X. P. Xing, Z. C. Tang. Reactions of platinum cluster ions with benzene. *Rapid Commun. Mass Spectrom.* **2006**, *20*, 1899.
[37] Z. X. Tian, Z. C. Tang. Experimental and theoretical studies of the interaction of silver cluster cations Ag_n^+ (n = 1–4) with ethylene. *Rapid Commun. Mass Spectrom.* **2005**, *19*, 2893.
[38] W. C. Wiley, I. H. McLaren. Time-of-flight mass spectrometer with improved resolution. *Rev. Sci. Instrum.* **1955**, *26*, 1150.
[39] H. Xie, X. Xing, Z. Liu, R. Cong, Z. Qin, X. Wu, Z. Tang, H. Fan. Probing the structural and electronic properties of Ag_nH^- (n = 1–3) using photoelectron imaging and theoretical calculations. *J. Chem. Phys.* **2012**, *136*, 184312.
[40] H. Xie, X. Li, L. Zhao, Z. Qin, X. Wu, Z. Tang, X. Xing. Photoelectron imaging and theoretical calculations of bimetallic clusters: $AgCu^-$, $AgCu_2^-$, and Ag_2Cu^-. *J. Phys. Chem. A* **2012**, *116*, 10365.
[41] Z. Liu, H. Xie, Z. Qin, R. Cong, X. Wu, Z. Tang, X. Lu, J. He. Vibrationally resolved photoelectron imaging of platinum carbonyl anion $Pt(CO)_n^-$ (n = 1–3): Experiment and theory. *J. Chem. Phys.* **2012**, *137*, 204302.
[42] M. A. Duncan. Invited review article: Laser vaporization cluster sources. *Rev. Sci. Instrum.* **2012**, *83*, 041101.
[43] C. Chi, J. Cui, Z. H. Li, X. Xing, G. Wang, M. Zhou. Infrared photodissociation spectra of mass selected homoleptic dinuclear iron carbonyl cluster anions in the gas phase. *Chem. Sci.* **2012**, *3*, 1698.
[44] Z. D. Reed, M. A. Duncan. Infrared spectroscopy and structures of manganese carbonyl cations, $Mn(CO)_n^+$ (n = 1–9). *J. Am. Soc. Mass Spectrom.* **2010**, *21*, 739.
[45] K. Hiraoka, T. Mori, S. Yamabe. On the formation of the isomeric cluster ions $(CO)_n^+$. *J. Chem. Phys.* **1991**, *94*, 2697.
[46] K. Hiraoka, T. Mori. Gas-phase stabilities of cluster ions $H^+(CO)_2(CO)_n$, $H^+(N_2)_2(N_2)_n$, and $H^+(O_2)_2(O_2)_n$ with n = 1–14. *Chem. Phys.* **1989**, *137*, 345.
[47] K. Hiraoka, M. Nasu, S. Fujimaki, E. W. Ignacio, S. Yamabe. Gas-phase stability and structure of the cluster ions $CF_3^+(CO)_n$, $CF_3^+(N_2)_n$, $CF_3^+(CF_4)_n$, and $CF_4H^+(CF_4)_n$. *J. Phys. Chem.* **1996**, *100*, 5245.
[48] F. Meyer, Y. M. Chen, P. B. Armentrout. Sequential bond-energies of $Cu(CO)_x^+$ and $Ag(CO)_x^+$ (x = 1–4). *J. Am. Chem. Soc.* **1995**, *117*, 4071.
[49] S. Goebel, C. L. Haynes, F. A. Khan, P. B. Armentrout. Collision-induced dissociation studies of $Co(CO)_x^+$ (x = 1–5): Sequential bond-energies and the heat of formation of $Co(CO)_4^+$. *J. Am. Chem. Soc.* **1995**, *117*, 6994.

